

# Effects of Compliant Ankles on Bipedal Locomotion

Thomas Schauß\*, Michael Scheint\*, Marion Sobotka\*, Wolfgang Seiberl<sup>§</sup>, and Martin Buss\*

\*Institute of Automatic Control Engineering, Technische Universität München, D-80290 München, Germany,  
schauss@tum.de, m.scheint@tum.de, marion.sobotka@tum.de, m.buss@ieee.org

<sup>§</sup>Department of Biomechanics in Sports, Technische Universität München, D-80290 München, Germany,  
wolfgang.seiberl@sp.tum.de

**Abstract**—The influence of ankle compliance on bipedal robot locomotion is investigated in this paper. The focus is on reduction of energy consumption. The concept of hybrid zero dynamics is adapted to design walking gaits with three phases: underactuated heel roll, full actuation and underactuated toe roll. Ankle springs work in parallel with the ankle actuators. Stiffness and offset of the linear torsional springs at the ankle and gait parameters are optimized simultaneously. It is shown that simultaneous optimization of spring properties and gait is superior to optimizing the spring after the gait. Optimal spring stiffness and offset lead to a major reduction in energy consumption. Furthermore, a more human-like gait is observed for simultaneous optimization of gait and spring parameters compared to gait optimization with zero stiffness.

## I. INTRODUCTION

Ongoing research on bipedal walking in the past decades resulted in legged robots with impressive versatility. Bipedes such as Asimo [1] or HRP-2 [2] can walk, climb stairs, and even run. Apart from versatility, desirable properties of a humanoid robot are low energy consumption and human-like walking motion. In comparison to human walking, energy efficiency of today's walking robots is mostly inferior [3]. Moreover, walking gaits of most bipedal robots only loosely resemble human gait.

A promising way to enhance energy efficiency of locomotion is to use springs. Fundamental possibilities of employing springs in locomotion were studied e.g. in [4]. Work at the actuators is reduced by energy storage and release through springs. In human walking, energy is stored elastically in the Achilles tendon around the ankle during controlled dorsiflexion and released at the end of the stance phase during powered plantarflexion [5].

The objective of this study is to mimic this single aspect of human anatomy and investigate the effects of adding a linear spring at the ankles in gait synthesis for walking. Energy storage and release of the ankle spring shall lead to an ankle push-off prior to heel strike, which is a known mechanism to reduce locomotion cost [5]. Overall, the aim is to reduce energy consumption and to obtain a more human like gait.

Compliant elements in biped robots that enable energy reduction have been studied previously in literature. One early example is the Waseda WL-14 [6], where energy efficiency was reported to improve by using a heuristically chosen hip spring. Recent research focused on the optimization of both, gait and spring properties, for improving energy efficiency. Spring stiffnesses and offsets were optimized along with gait

in [7], [8], but restrictions on the admissible gait such as step length in [7] were imposed. In [8] only fully actuated walking was considered. Gait, spring offset, and spring preload were optimized for a set of knee stiffnesses in [9]. In [10], passive ankles of a biped were equipped with springs. Cost of flat foot walking was reduced through optimization of gait and spring stiffness. For all the aforementioned examples, energy consumption of locomotion was reduced to some extent through the springs, but a more natural looking gait was not necessarily obtained.

The research presented here differs from the above studies in two main aspects. First, restrictions on gait are kept to a minimum. Specifying step length or intermediate poses as in [7] narrows the search space of the gait optimization and is prone to deliver suboptimal gaits. Second, the gait and all spring properties are simultaneously optimized with respect to energy consumption. The underlying hypothesis is that only the combination of these two aspects allows to find a suitable gait-spring combination that takes full advantage of the energy storage and release mechanism of the spring. This energy optimal gait is expected to more closely resemble human walking. The same approach was applied before for a 5-link biped with leg compliance and point feet [11].

In particular, this study focuses on the effects of a linear spring in parallel with the ankle of a 7-link biped with feet. The walking motion in single support consists of up to three phases: heel roll, full actuation, and toe roll. The duration of the respective phases is a gait parameter and subject to optimization. The method of hybrid zero dynamics [12] is applied to obtain stable gaits with alternating underactuated and fully actuated phases. Simulations of the resulting biped gaits are compared to human gait data.

The remainder of the paper is structured as follows. Section II introduces the model of the 7-link biped. Section III gives a brief review of the method of hybrid zero dynamics for walking with flat feet. Section IV defines the resulting optimization problem. Section V discusses simulation results with respect to energy consumption. In section VI, simulation of optimized gait is compared to recorded human gait data. Section VII draws a conclusion.

## II. MODEL

The 7-link biped under study is depicted in Figure 1. The feet are anthropomorphic with a flat sole. Only motion in the sagittal plane is allowed. Desired gaits consist of several

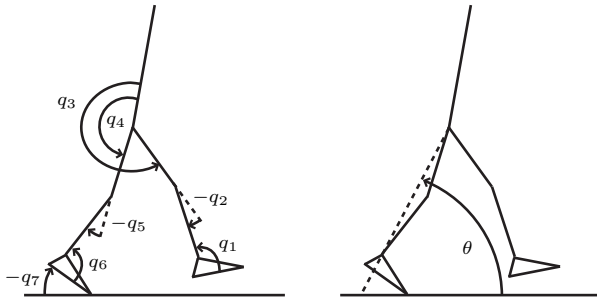


Fig. 1. Kinematics of the biped.  $q_1$  to  $q_6$  are the body angles of the biped where torques  $u_1$  to  $u_6$  act,  $q_7$  is not actuated. The upper body link substitutes head, arms, and torso. For the HZD, coordinate  $\theta$  is defined as the angle of the connecting line between ankle and hip.

contact phases, separated by instantaneous transitions. During single support, the foot that contacts the walking surface is called stance foot, the other swing foot.

A step starts with underactuated heel roll where only the heel of the stance foot has ground contact. After toe impact, a phase with full actuation follows, where the stance foot is flat on the ground. The subsequent heel lift is followed by underactuated toe roll where only the toe of the stance foot has ground contact. After toe roll, heel impact occurs. The former stance foot becomes the new swing foot and vice versa. Impacts are modeled as instantaneous and perfectly inelastic. This includes the double support phase, i.e. directly after heel impact the new swing foot loses contact with the walking surface.

The state of the control system consists of the coordinates  $\mathbf{q} = [q_1 \ q_2 \ q_3 \ q_4 \ q_5 \ q_6 \ q_7]^T$  and their angular velocities  $\dot{\mathbf{q}} = [\dot{q}_1 \ \dot{q}_2 \ \dot{q}_3 \ \dot{q}_4 \ \dot{q}_5 \ \dot{q}_6 \ \dot{q}_7]^T$ . During full actuation the coordinate  $q_7$  and its angular velocity  $\dot{q}_7$  are zero. Masses are distributed over the links. The joints are massless and frictionless. The actuators in the joints are modeled as ideal, i.e. they are massless, frictionless, and discontinuities in the torques are allowed. To shorten notation, continuous phases and transitions are defined generally for phase  $i$  and  $j$ . The phases  $i$  and  $j$  are substitutes for  $h$  (heel roll),  $f$  (full actuation), or  $t$  (toe roll). Models in minimal coordinates can be determined using the Euler-Lagrange equation as

$$D_i(\mathbf{q}_i)\ddot{\mathbf{q}}_i + C_i(\mathbf{q}_i, \dot{\mathbf{q}}_i)\dot{\mathbf{q}}_i + \mathbf{g}_i(\mathbf{q}_i) = \mathbf{B}_i\mathbf{u}, \quad (1)$$

where  $i \in \{h, f, t\}$ ,  $D_i$  is the mass-inertia matrix,  $C_i$  summarizes centrifugal and Coriolis effects,  $\mathbf{g}_i$  summarizes forces and torques generated by gravity, and  $\mathbf{B}_i$  is the control matrix. The minimal coordinates of the underactuated phases are  $\mathbf{q}_h = \mathbf{q}_t = \mathbf{q}$  and for the fully actuated phase  $\mathbf{q}_f = [q_1 \ q_2 \ q_3 \ q_4 \ q_5 \ q_6]^T$ .

In state space form the dynamic model of phase  $i$  is

$$\dot{\mathbf{x}}_i = \mathbf{f}_i(\mathbf{x}_i) + \mathbf{G}_i(\mathbf{x}_i)\mathbf{u} \quad \text{with } i \in \{h, f, t\}. \quad (2)$$

The state spaces of the system in which  $\mathbf{q}_h$ ,  $\mathbf{q}_f$ , and  $\mathbf{q}_t$  are restricted to valid values  $\mathcal{Q}_i$  are

$$\mathcal{X}_i = \left\{ \mathbf{x}_i = \left[ \mathbf{q}_i^T \ \dot{\mathbf{q}}_i^T \right]^T \mid \mathbf{q}_i \in \mathcal{Q}_i \subset \mathbb{R}^{N_i}, \ \dot{\mathbf{q}}_i \in \mathbb{R}^{N_i} \right\},$$

with  $i \in \{h, f, t\}$ ,  $N_h = N_t = N = 7$ , and  $N_f = N - 1 = 6$ .

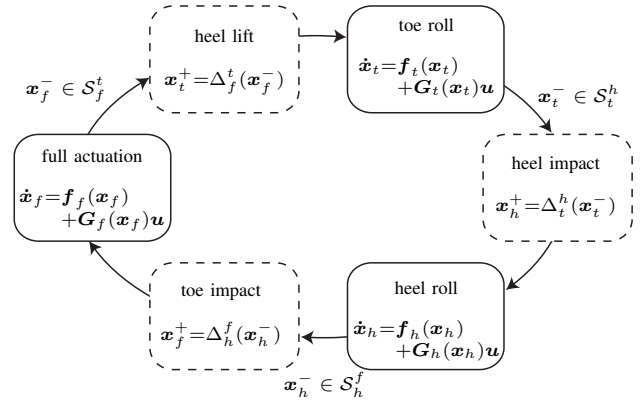


Fig. 2. States and transitions of hybrid model of walking. Solid boxes depict discrete states, dashed boxes depict instantaneous transitions.

It is assumed that springs and actuators act in parallel, therefore the spring dynamics can be seen as additional input. The total torque  $\mathbf{u}$  applied at the joints then is

$$\begin{aligned} \mathbf{u} &= \mathbf{u}_{\text{ext}} + \mathbf{u}_{\text{el}} \\ &= \mathbf{u}_{\text{ext}} + K \begin{bmatrix} (q_1 - q_{\text{off}}) & \mathbf{0}^{1 \times 4} & (q_6 - q_{\text{off}}) \end{bmatrix}^T, \end{aligned} \quad (3)$$

where  $\mathbf{u}_{\text{ext}}$  is the externally applied motor torque and  $\mathbf{u}_{\text{el}}$  is the torque applied by the springs. The stiffness of the springs is denoted by  $K$  and the offset angle is denoted by  $q_{\text{off}}$ .

Switching surfaces  $S_h^f$ ,  $S_f^t$ , and  $S_t^h$  of dimensions  $N - 1$ ,  $N - 2$ , and  $N - 1$  are defined. The switching surface  $S_f^t$  determines the set of states where heel lift is initiated. This transition is subject to optimization. The switching surface  $S_t^h$  specifies contact of the swing heel with the ground. The switching surface  $S_h^f$  is used to determine contact of the stance foot toe with the ground. Impact maps can be derived from the extended model. Only for heel lift no discontinuities in angles or angular velocities appear. For the transition from phase  $i$  to phase  $j$  a reset map can be written as

$$\mathbf{x}_j^+ = \Delta_i^j(\mathbf{x}_i^-) \quad \text{for } \mathbf{x}_i^- \in S_i^j, \quad (4)$$

where  $\mathbf{x}_i^-$  is the state directly before the transition,  $\mathbf{x}_j^+$  is the state directly after the transition, and  $(i, j) \in \{(h, f), (f, t), (t, h)\}$ .

Combining equations (2) and (4) yields the hybrid model of the complete system:

$$\Sigma : \begin{cases} \dot{\mathbf{x}}_i = \mathbf{f}_i(\mathbf{x}_i) + \mathbf{G}_i(\mathbf{x}_i)\mathbf{u} & \mathbf{x}_i^- \notin S_i^j \\ \mathbf{x}_j^+ = \Delta_i^j(\mathbf{x}_i^-) & \mathbf{x}_i^- \in S_i^j \end{cases}, \quad (5)$$

with  $(i, j) \in \{(h, f), (f, t), (t, h)\}$ . A summary of discrete states and transitions is given in Figure 2.

### III. CONTROL

The desired walking gait contains contact phases in which the biped is underactuated (heel roll, toe roll). In order to cope with this difficulty, the concept of hybrid zero dynamics (HZD) developed by Westervelt *et al.* [12] is used here. It allows the systematic design and optimization of a feedback controller for bipedal walking using virtual constraints. The orbital stability of the limit cycle can be tested on a reduced system dynamics of dimension two.

In this section the main ideas of [12] are briefly presented including some modifications. To shorten notation the indices of the different phases are omitted where possible. The concept is shown here only for the underactuated phases. The design procedure of the hybrid zero dynamics starts with the definition of a set of output functions, called virtual constraints, for each phase. A feedback linearizing controller is derived for these constraints leading to zero dynamics. It is shown, how the output function is parametrized for later optimization and how a closed orbit and a hybrid zero dynamics can be constructed. Finally, the extension of [12] towards additional heel roll and the incorporation of springs are presented.

In order to construct a HZD, virtual holonomic constraints are imposed on the directly actuated joints  $\mathbf{q}_b$  (i.e. body angles) of the biped. To this end, a function  $\mathbf{h}_d(\theta, \gamma)$  of an unactuated coordinate  $\theta$  and a parameter vector  $\gamma$  is defined. The function  $\mathbf{h}_d(\theta, \gamma)$  is not directly time dependent. The unactuated coordinate  $\theta$  must be strictly monotonic decreasing for each continuous phase and its choice is shown in Figure 1. Then an output function  $\mathbf{h}(\mathbf{q}) = \mathbf{q}_b - \mathbf{h}_d(\theta, \gamma)$  is defined for each phase. With input/output linearizing state feedback and an appropriate controller  $\mathbf{v}(\mathbf{x})$ , an input  $\mathbf{u}(\mathbf{x})$  can be determined driving the output function  $\mathbf{h}(\mathbf{q})$  to zero:

$$\mathbf{u}(\mathbf{x}) = (L_f L_G \mathbf{h}(\mathbf{q}))^{-1} (\mathbf{v}(\mathbf{x}) - L_f^2 \mathbf{h}(\mathbf{q})). \quad (6)$$

The output function  $\mathbf{h}(\mathbf{q})$  is controlled by  $\mathbf{v}(\mathbf{x})$ , i.e.

$$\frac{d^2}{dt^2} \mathbf{h}(\mathbf{q}) = \mathbf{v}(\mathbf{x}).$$

On the zero dynamics, i.e. when the output function  $\mathbf{h}(\mathbf{q})$  and its derivative  $L_f \mathbf{h}(\mathbf{q})$  are zero, the input (6) becomes

$$\mathbf{u}^*(\mathbf{x}) = -(L_f L_G \mathbf{h}(\mathbf{q}))^{-1} L_f^2 \mathbf{h}(\mathbf{q}). \quad (7)$$

Applying this input renders the output function  $\mathbf{h}(\mathbf{q})$  forward invariant for any starting value  $\mathbf{z}$  with

$$\mathbf{z} \in \mathcal{Z} = \{\mathbf{x} \mid \mathbf{h}(\mathbf{q}) = \mathbf{0}, L_f \mathbf{h}(\mathbf{q}) = \mathbf{0}\}.$$

Then the dynamics of the system can be denoted

$$\dot{\mathbf{z}} = \mathbf{f}(\mathbf{z}) + \mathbf{G}(\mathbf{z}) \mathbf{u}^*(\mathbf{z}) \in \mathcal{T}_z \mathcal{Z}, \quad (8)$$

and the state  $\mathbf{z}$  is constrained to the set  $\mathcal{Z}$  for all times. These reduced dynamics (8) are called zero dynamics.

The constraints  $\mathbf{h}_d(\theta, \gamma)$  are designed in such a way, that the output function becomes transition invariant, i.e. if  $\mathbf{q}_b$  and  $\dot{\mathbf{q}}_b$  are constraint admissible before impact they are also constraint admissible after impact,

$$\Delta_i^j (\mathcal{S}_i^j \cap \mathcal{Z}_i) \subset \mathcal{Z}_j, \quad (9)$$

with  $(i, j) \in \{(h, f), (f, t), (t, h)\}$ . Forward invariance and transition invariance result in hybrid invariance. The unactuated dynamics of such a system are called hybrid zero dynamics (HZD). In this case the HZD is a first order system of dimension two. The state variables are the angle  $\theta$  and the angular momentum conjugate to  $\theta$ , which is denoted by  $\sigma$ . On the HZD the state of the complete system can be determined from the state of the HZD.

The properties of the limit cycle of the HZD are determined by the choice of the function  $\mathbf{h}_d(\theta, \gamma)$ . Here, the components of  $\mathbf{h}_d$  are chosen to be Bézier polynomials of order six. The first two coefficients of each Bézier polynomial are determined by the transition maps such that the output functions become transition invariant. The five remaining coefficients of each Bézier polynomial and the angle  $\theta_f$  where heel lift occurs represent the degrees of freedom for gait design, and are summarized in the parameter vector  $\gamma$ .

The main difference to [12] is the additional heel roll phase. Adding this phase to the control framework is a straightforward extension as it is similar to toe roll.

To incorporate the springs and compute the motor torques  $\mathbf{u}_{\text{ext}}^*$  on the limit cycle, first the torques  $\mathbf{u}^*$  necessary to render the HZD forward invariant are computed using the input/output linearization (7). The torques applied by the springs  $\mathbf{u}_{\text{el}}^*$  then are subtracted:

$$\mathbf{u}_{\text{ext}}^* = \mathbf{u}^* - \mathbf{u}_{\text{el}}^*. \quad (10)$$

#### IV. OPTIMIZATION

Optimization is used to search for a gait which is determined by the parameters in  $\gamma$ . The stiffness  $K$  and offset angle  $q_{\text{off}}$  of the springs do not directly alter the gait but will influence the cost of locomotion. Therefore, gait is optimal if it also enables beneficial operation of the springs. Different optimal gait parameters are determined by simultaneous optimization of gait and spring in comparison to optimization of only gait parameters.

The nonlinear optimization problem for finding appropriate gaits based on the HZD method has a nonlinear equality constraint  $c_e$  and nonlinear inequality constraints  $c_i$ :

$$\min_{\gamma \in \Gamma} J(K, q_{\text{off}}, \gamma) \quad (11)$$

$$K \in \mathbb{R}^+, q_{\text{off}} \in [-\pi, \pi]$$

$$\text{with } \Gamma = \{\gamma \in \mathbb{R}^M, c_e(\gamma) = 0, c_i(\gamma) \leq 0\}. \quad (12)$$

Here,  $M = 90$  is the number of free gait parameters in  $\gamma$ . The constraints  $c_e(\gamma)$ ,  $c_i(\gamma)$  are defined below.

This research considers the effects of springs in an idealized model and some assumptions have already been made for the motors (massless, frictionless). Therefore, also gears are neglected as it is common in research on gait synthesis and optimization. The energy consumption of a DC motor can then be approximated as the square of the current  $I^2$ . The current  $I$  is roughly proportional to the torque acting at the motor shaft. The torques applied externally at the joints on the hybrid zero dynamics are  $\mathbf{u}_{\text{ext}}^*(t, K, q_{\text{off}}, \gamma)$ . Consequently, for this model a cost function that is an estimation of energy consumption, normalized by traveled distance, can be defined as

$$J(K, q_{\text{off}}, \gamma) = \frac{1}{L_s(\gamma)} \int_0^{T_s(\gamma)} \|\mathbf{u}_{\text{ext}}^*(t, K, q_{\text{off}}, \gamma)\|_2^2 dt. \quad (13)$$

The step time  $T_s$  and the step length  $L_s$  can be computed from the gait parameters  $\gamma$ .

TABLE I

RESULTS OF OPTIMIZATION. DESIRED WALKING SPEED  $v_{\text{des}}$  IS 1.5 m/s. THE TABLE LISTS COST OF LOCOMOTION  $J$ , STEP-TIME  $T_s$ , STEP-LENGTH  $L_s$ , AND SPRING PARAMETERS  $K$  AND  $q_{\text{off}}$ .

	Case	Description	$J$	$L_s$	$K$	$q_{\text{off}}$
		Unit	$\text{N}^2\text{ms}$	m	Nm	-
3 Phases	A3	3 phases, simultaneous opt. of gait and spring	219	0.84	450	1.55
	B3	3 phases, opt. of gait, no spring	2757	0.75	0	-
	C3	3 phases, opt. of gait, then spring	2755	0.75	1.79	1.34
2 Phases	A2	2 phases, simultaneous opt. of gait and spring	105	0.86	319	1.68
	B2	2 phases, opt. of gait, no spring	2705	0.53	0	-
	C2	2 phases, opt. of gait, then spring	2653	0.53	21.6	1.31

The equality constraint  $c_e(\gamma)$  is used to achieve a desired average forward velocity  $v_{\text{des}}$  of the biped. It is defined as

$$c_e(\gamma) = v_{\text{des}} - \frac{L_s(\gamma)}{T_s(\gamma)}. \quad (14)$$

There are different types of inequality constraints in  $c_i(\gamma)$ . On the one hand there are constraints necessary for the existence of the hybrid zero dynamics. E.g. the angular momentum  $\sigma$  must be negative for all times. On the other hand there are constraints which assure that a valid gait is generated. The swing foot must be above the walking surface during single support and one stance foot edge must be above the walking surface during underactuated phases. During the fully actuated phase the stance foot must stay flat on the ground, i.e. the foot rotation indicator (FRI) must be within the foot support area. The FRI is the point at which the vertical ground reaction force has to act, to keep the foot from tipping over one of the foot edges [13]. Furthermore, as in human anatomy, the knees are constrained to bend backwards only. In addition, there are constraints on the contact forces depending on the chosen friction coefficient.

It is important to note, that there are no artificial constraints on step length, step time, height of the swing foot above the ground, angle of the upper body, minimum height of the hips, joint angle of ankle, etc.

In the following section, walking with three phases and elasticities is compared to a simpler walking gait and to walking without springs. By applying slight modifications to control and optimization, a gait with only two phases (full actuation, toe roll) can be determined. Optimization with constant spring parameters (or no spring) is straightforward.

## V. RESULTS

In this section characteristics of optimal gait are compared for different modeling assumptions. The link lengths, masses, centers of mass, and moments of inertia are the same for all models and are based on anthropomorphic data from [14]. The biped has a height of 1.80 m and a weight of 75.0 kg.

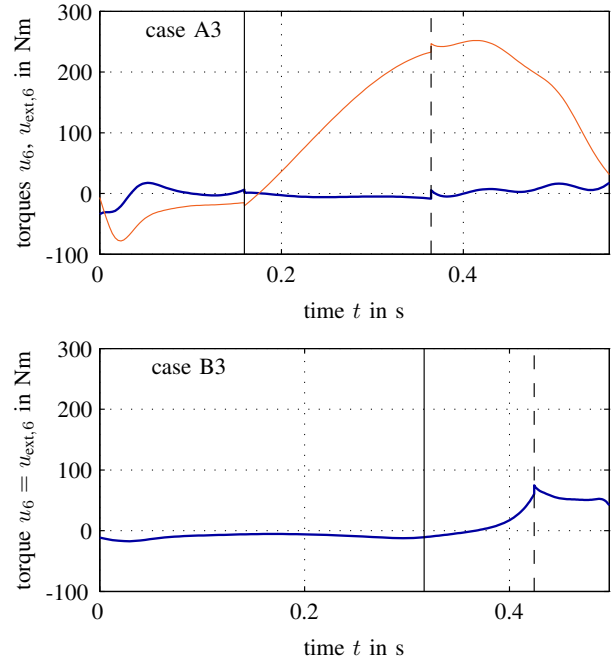


Fig. 3. Stance ankle torques for one step (heel impact to next heel impact). Case A3 optimized with ankle springs and case B3 without springs. Total torques (red) and motor torques (blue, bold) at the ankle joint are compared. For case B3 motor torques and total torques are identical. Toe impact is marked by a solid vertical line, heel lift is marked by a dashed vertical line.

Cost of locomotion, step length, step time, and spring parameters are shown in Table I for two different models (3 phase gait and 2 phase gait). Further, simultaneous optimization of gait and springs is compared to optimization of gait only and to successive optimization of gait and springs. In the latter case, it is investigated to what extent optimal springs can help to improve energy efficiency of an existing gait pattern.

It is found, that successive optimization of gait and springs leads only to a slight reduction of the cost of locomotion (compare case C3 to case B3 and case C2 to case B2) while optimizing spring and gait simultaneously results in a reduction of the cost of locomotion by an order of magnitude (compare case A3 to case B3 and case A2 to case B2). Also, simultaneous optimization of gait and spring results in springs with higher stiffness, because a gait is determined that can optimally utilize the spring in the ankle. Here, the cost of locomotion for a gait with two phases is lower than the respective cost for a gait with three phases. Nevertheless, it is believed that a minimum with even lower cost for the gait with three phases exists that has a very short heel roll phase. However, due to the chosen concept very short phases result in poor convergence of the numerical optimization and better gaits could not be found.

Figure 3 depicts the total torque in comparison to the motor torque at the stance ankle for the gait with and without springs (cases A3 and B3). Although the average and maximum motor torque is significantly smaller for the gait with ankle springs (case A3), a larger average and maximum total torque acts at the stance ankle joint. The gait was optimized, as to best utilize the effect of the spring in the ankle. Therefore, the optimal solution found for the model

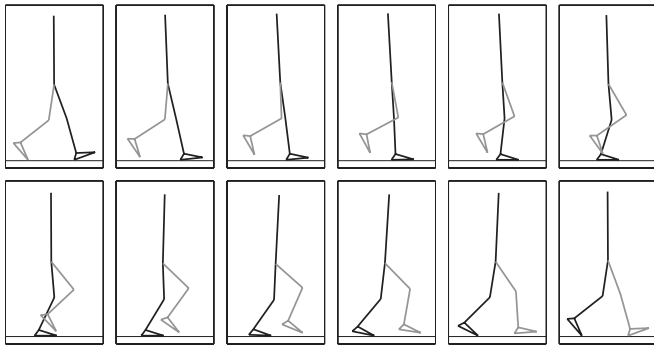


Fig. 4. Snapshots of gait (case A3). Time between two snapshots is  $1/11 T_s$ . The stance leg is plotted in black, the swing leg in gray. Average forward velocity is 1.5 m/s.

with ankle springs (A3) can not be the optimal solution for the model without ankle springs (B3).

Figure 4 shows one step of the gait with simultaneously optimized gait and spring (case A3), whereas the gait without spring action (case B3) is depicted in Figure 6. Note, that successive optimization of spring parameters for a fixed gait will not alter the shape of the trajectory. Qualitative analysis yields, that the gait after simultaneous optimization (case A3) is generally more smooth. In case of simultaneous optimization (case A3) the three phases are of similar duration (28 %, 37 %, and 35 %). For the gait without springs (case B3) heel roll, full actuation, and toe roll account for 64 %, 21 %, and 15 % of the step respectively. Furthermore, an unnatural angle of the swing leg ankle is observed and the upper body is lent forward during the complete step for the gait without springs (case B3). A comparison of different characteristics of those gaits with recorded human gait data is shown in the next section.

The numerical optimization scheme used to determine the optimal gaits can only obtain local minima. Thus, it must be validated that the reduction in cost when optimizing spring and gait simultaneously is really caused by the spring. Figure 5 shows the optimal cost of locomotion for the gait with two phases for different fixed spring parameters. This cost is monotonically increasing around the minimum obtained by optimizing gait and spring simultaneously. Furthermore, the

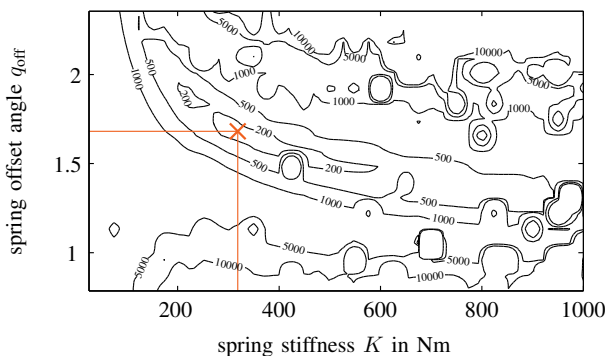


Fig. 5. Cost of locomotion of optimal gait with two phases for different spring parameters. Average forward velocity is 1.5 m/s. The optimal solution for simultaneous optimization of spring and gait (case A2) is marked by a cross. Data interpolated from a 760 points grid. For some spring parameters optimization did not converge resulting in very high cost of locomotion.

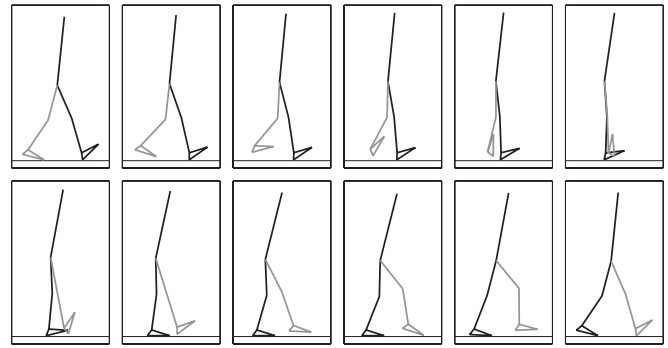


Fig. 6. Snapshots of gait (case B3/C3). Time between two snapshots is  $1/11 T_s$ . The stance leg is plotted in black, the swing leg in gray. Average forward velocity is 1.5 m/s.

gradient of costs is smooth between the solution of case A2 (marked by the cross) and case B2 ( $K = 0$ ). Thus it can be concluded, that the two solutions have the same region of attraction and the difference in cost is caused by optimizing spring and gait parameters simultaneously.

## VI. COMPARISON WITH HUMAN GAIT DATA

In order to assess how human like the optimized biped walking gait is, simulation data of the biped is compared to human gait data. It has to be noted, that the biped motion is restricted to the sagittal plane. Comparison of this biped motion with a projection of human motion onto the sagittal plane is common practice. For the robot, two cases (A3 and B3) with three phases are used for this comparison. Although three phase walking has a higher cost than two phase walking, the latter is not selected for comparison as the missing heel phase alters the impact at touchdown and hence leads to noticeable different force characteristics.

The human kinematic data was captured at the Dept. of Biomechanics in Sports, TU München. Walking trials were performed by 14 healthy male subjects (mean age  $25.3 \pm 2.7$  years, BMI  $23.5 \pm 1.9 \text{ kg/m}^2$ ). Gait was analyzed using a VICON optical tracking system with 240 Hz and a Kistler force plate with 480 Hz. In the following, two features of a walking gait are considered: ground reaction force (GRF) and stance ankle torque. For each feature, human walking data was first interpolated to a mutual time vector and then averaged over all valid test trials.

The vertical and horizontal GRF component at the stance foot are shown in Figure 7. Concerning the horizontal component, the simulation data for both cases of the biped follow the human GRF data to the same extent. As neither case A3 nor case B3 can be regarded as more human-like, an ankle spring seems not to have an effect here.

For the vertical GRF, a clear difference between case A3 with ankle spring and case B3 without can be seen. In case A3, the vertical force shows the typical “M”-like shape. Compared to the human gait data, the first peak is too early and both peaks have a higher value. The vertical GRF for the biped without ankle spring shows a clearly different course, with a very high and distinct peak just before heel rise.

Figure 8 shows the stance ankle torque over one step. It can be seen, that for case A3 with ankle spring the

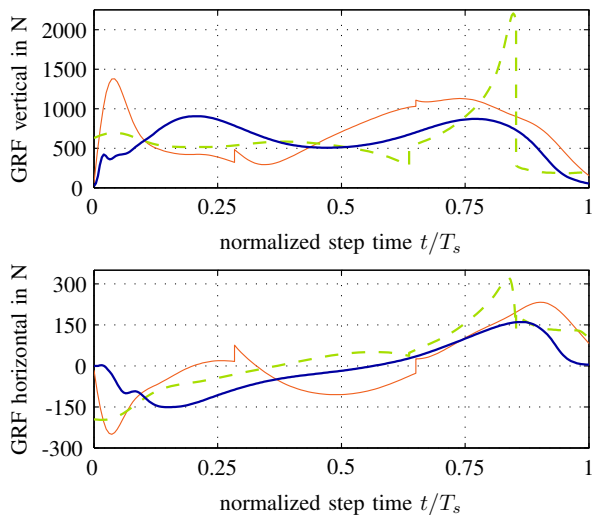


Fig. 7. Ground reaction force (GRF) over one step for human (blue, bold), biped case A3 (red, solid), and biped case B3 (green, dashed). Top plot shows vertical component of GRF, lower plot horizontal component.

characteristics of the ankle torque are similar to the human case. After the initial negative torque region, torque rises rather steadily to a peak at approx. 75% of step time, followed by a descent towards zero. For case B3 without ankle spring, torque is negative throughout most time of the step and rises sharply to the peak, resulting in a course being qualitatively different from the human case.

However, it has to be noted, that the maximum torque values differ (case A3: 3.36 Nm/kg, case B3: 1.00 Nm/kg, human: 1.60 Nm/kg). One possible explanation for the high value of case A3 is that optimization favored ankle actuation which can be performed by the spring without cost.

Summarizing the comparison, it can be concluded that for certain gait features the biped walking gait is more human-like when gait and ankle spring are simultaneously optimized for energy consumption. Noticeable variations e.g. in the vertical GRF can be attributed to the missing non-instantaneous double support phase, the approximation of the elastic behavior of the human ankle by a linear spring, missing compliant elements in the other joints and the use of a 2D model for the biped.

## VII. CONCLUSION

Optimal gait planning was presented for a 7-link robot with compliant ankle using the hybrid zero dynamics method. For one step consisting of heel roll, full actuation, and toe roll, gait and spring properties were optimized simultaneously. In comparison to walking without compliant elements, cost could be reduced by one order of magnitude. A comparable reduction of cost can not be achieved when optimizing the spring parameters after optimizing gait. In addition, the gait with three contact phases and ankle compliance was found to have strong similarities with human gait. This is confirmed by comparison with recorded human walking data. Future research will investigate the role of the double support phase on energy consumption and optimal gait.

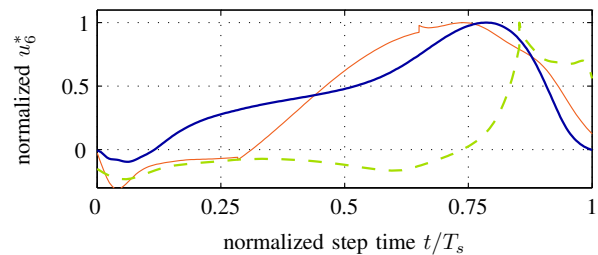


Fig. 8. Stance ankle torque over one step for human (blue, bold), biped case A3 (red, solid), and biped case B3 (green, dashed). Ankle torque is normalized by its respective maximum value.

## VIII. ACKNOWLEDGMENTS

This work is supported in part within the Grant WO1440/2-1 of the German Research Foundation (DFG). The authors thank Michelle Karg for her help on the analysis of the gait measurement data.

## REFERENCES

- [1] Y. Sakagami, R. Watanabe, C. Aoyama, S. Matsunaga, N. Higaki, and K. Fujimura, "The intelligent ASIMO: system overview and integration," in *Proceedings of the IEEE/RSJ International Conference on Intelligent Robots and System (IROS)*, vol. 3, 2002, pp. 2478–2483.
- [2] K. Kaneko, F. Kanehiro, S. Kajita, H. Hirukawa, T. Kawasaki, M. Hirata, K. Akachi, and T. Isozumi, "Humanoid robot HRP-2," in *Proceedings of the IEEE International Conference on Robotics and Automation (ICRA)*, vol. 2, 2004, pp. 1083–1090.
- [3] S. Collins, A. Ruina, R. Tedrake, and M. Wisse, "Efficient bipedal robots based on passive-dynamic walkers," *Science*, vol. 307, no. 5712, pp. 1082–1085, 2005.
- [4] R. M. Alexander, "Three uses for springs in legged locomotion," *The International Journal of Robotics Research*, vol. 9, no. 2, pp. 53–61, 1990.
- [5] A. Kuo, "Choosing your steps carefully," *IEEE Robotics & Automation Magazine*, vol. 14, no. 2, pp. 18–29, 2007.
- [6] J. Yamaguchi, D. Nishino, and A. Takaniishi, "Realization of dynamic biped walking varying joint stiffness using antagonistic driven joints," in *Proceedings of the IEEE International Conference on Robotics and Automation (ICRA)*, vol. 3, 1998, pp. 2022–2029.
- [7] V. Duindam and S. Stramigioli, "Optimization of mass and stiffness distribution for efficient bipedal walking," in *Proceedings of the International Symposium on Nonlinear Theory and its Applications*, Bruges, Belgium, 2005.
- [8] K. D. Mombaur, R. W. Longman, H. G. Bock, and J. P. Schlöder, "Optimizing spring-damper design in human like walking that is asymptotically stable without feedback," in *Modeling, Simulation and Optimization of Complex Processes*. Springer, 2008, pp. 403–418.
- [9] T. Yang, E. Westervelt, and J. Schmiedeler, "Using parallel joint compliance to reduce the cost of walking in a planar biped robot," in *Proceedings of the 2007 ASME International Mechanical Engineering Congress and Exposition*, Seattle, 2007.
- [10] K. Farrell, C. Chevallereau, and E. Westervelt, "Energetic effects of adding springs at the passive ankles of a walking biped robot," in *Proceedings of the IEEE International Conference on Robotics and Automation (ICRA)*, 2007, pp. 3591–3596.
- [11] M. Scheint, M. Sobotka, and M. Buss, "Compliance in gait synthesis: Effects on energy and gait," in *Proceedings of the IEEE International Conference on Humanoid Robots*, Daejeon, Korea, 2008, pp. 259–264.
- [12] E. Westervelt, J. Grizzle, C. Chevallereau, J. H. Choi, and B. Morris, *Feedback Control of Dynamic Bipedal Robot Locomotion*. CRC Press, 2007.
- [13] A. Goswami, "Foot rotation indicator (FRI) point: a new gait planning tool to evaluate postural stability of biped robots," in *Proceedings of the IEEE International Conference on Robotics and Automation (ICRA)*, vol. 1, 1999, pp. 47–52.
- [14] D. A. Winter, *Biomechanics and Motor Control of Human Movement, Second Edition*. John Wiley & Sons, Inc., 1990.